J Mol Model (2011) 17:543–553
DOI 10.1007/s00894-010-0748-y

ORIGINAL PAPER

Molecular modeling of lanthionine synthetase component C-like protein 2: a potential target for the discovery of novel type 2 diabetes prophylactics and therapeutics

Pinyi Lu · David R. Bevan · Stephanie N. Lewis · Raquel Hontecillas · Josep Bassaganya-Riera

Received: 30 March 2010 / Accepted: 6 May 2010 / Published online: 30 May 2010

Abstract The rates of type 2 diabetes (T2D) are rising to epidemic proportions in the US and worldwide. While current T2D medications are efficacious, significant side effects have limited their use and availability. Our laboratory has discovered that abscisic acid (ABA) exerts anti-diabetic effects, in part, by activating peroxisome proliferator-activated receptor γ (PPAR γ). However, since ABA does not bind to the ligand-binding domain (LBD) of PPAR γ, the mechanism of activation of PPAR γ by ABA remains unknown. Lanthionine synthetase component C-like protein 2 (LANCL2) was predicted to be a novel target for the binding and signaling of ABA in human granulocytes and rat insulinoma cells. The goal of this study was to determine whether LANCL2 is a molecular target of ABA and other PPAR γ agonists. To this end we performed homology modeling to construct a three-dimensional structure of LANCL2 using the crystal structure of LANCL1 as a template. Our molecular docking studies predicted that ABA and other PPAR γ agonists (e.g., rosiglitazone and pioglitazone) share a binding site on the surface of LANCL2. The identification of a binding site for PPAR γ agonists will facilitate the high-throughput virtual screening of large compound libraries and may shed new light on alternative mechanisms of PPAR γ activation.

Keywords Lanthionine synthetase component C-like protein 2 · Homology modeling · Docking · Abscisic acid · Type 2 diabetes · Thiazolidinediones

P. Lu · S. N. Lewis
Genetics, Bioinformatics, and Computational Biology Program,
Virginia Polytechnic Institute and State University,
Blacksburg, VA 24061, USA

P. Lu · S. N. Lewis · R. Hontecillas · J. Bassaganya-Riera (✉)
Nutritional Immunology and Molecular Nutrition Laboratory,
Virginia Bioinformatics Institute,
Virginia Polytechnic Institute and State University,
Washington Street 0477,
Blacksburg, VA 24061, USA
e-mail: jbassaga@vt.edu

P. Lu · D. R. Bevan · S. N. Lewis
Department of Biochemistry,
Virginia Polytechnic Institute and State University,
201 Engel Hall 0308,
Blacksburg, VA 24061, USA

Introduction

According to recent estimates from the Centers for Disease Control and Prevention (CDC), about 30% of the United States population is obese and 65% is overweight. One of the major consequences of these high rates is manifested by the increased prevalence of type 2 diabetes mellitus (T2D), a disorder that is characterized by high blood glucose in the context of insulin resistance that progresses towards pancreatic β-cell dysfunction leading to insulin deficiency [1]. There are an estimated 23.6 million people in the US (7.8% of the population) with diabetes, 90% of whom are type 2 diabetics [2]. With prevalence rates doubling between 1990 and 2005, CDC has characterized this increase as an epidemic.

Current antidiabetic drugs used in the management of T2D elicit important insulin-sensitizing and anti-inflammatory effects. However, side effects associated with using these medications are serious, any of which may limit their use [3]. For example, sulfonylureas, the first widely used oral hypoglycemic medications, cause hypoglycemia [4]; biguanides are typically reserved for patients experiencing gastrointestinal side effects [5] and thiazolidinediones (TZDs) could lead to an increase in the incidence of liver damage and potential liver failure, fluid retention, weight

gain and congestive heart failure [6]. Thus, it is critical to discover novel, naturally occurring drugs and nutraceuticals against T2D.

Our laboratory is actively screening and discovering novel, naturally occurring, orally active nutraceuticals against diabetes, cardiovascular disease, gut inflammation and inflammation-driven cancer that activate nuclear receptors. Of note is the discovery of a peroxisome proliferator-activated receptor (PPAR) γ-activating and anti-inflammatory phytohormone, abscisic acid (ABA), which is also a potent insulin-sensitizing agent. PPAR γ is one of three PPAR isoforms (α, δ, and γ) that is a component of an extensive group of transcription factors controlling adipogenesis and glucose homeostasis, and both of these processes directly affect obesity and T2D [7]. ABA is a phytochemical regulating fundamental physiological functions in plants but it can also be endogenously synthesized in mammalian cells, including granulocytes, pancreatic β-cells and monocytes [8].

PPAR γ is required for ABA to induce its full spectrum of effects [9], but our unpublished data indicate that ABA does not bind directly to the ligand-binding domain (LBD) of PPAR γ. Therefore, the complete mechanism of activation of PPAR γ by ABA is unknown. Recently, Sturla and his colleagues provided in vitro results suggesting that the lanthionine synthetase component C-like protein 2 (LANCL2) is the membrane receptor required for ABA binding on the membrane of human granulocytes, and that LANCL2 is necessary for transduction of the ABA signal into cell-specific functional responses in granulocytes [10]. LANCL2 is a member of the eukaryotic lanthionine synthetase component C-Like (LANCL) protein family, which is related to the bacterial lanthionine synthetase component C [11] and is a putative novel target for the discovery and development of drugs and nutraceuticals.

In order to further understand the function of LANCL2 through its structure and to investigate whether ABA activates LANCL2 via direct binding to its extracellular domain, we performed homology modeling of human LANCL2 using the crystal structure of human lanthionine synthetase component C-like protein 1 (LANCL1) as a template [12], assessed the model quality and refined the model through energy minimization procedures. We then used a blind docking approach to elucidate the location of the potential LBD of LANCL2 for ABA. Docking results were evaluated by investigating the interaction of multiple ABA conformations with LANCL2. We also tested whether other synthetic and naturally occurring agonists of PPAR γ could bind to LANCL2 by blind docking. Interestingly, we found that these PPAR γ agonists could bind to the binding region of LANCL2 we propose is occupied by ABA. Among the tested ligands, thiazolidinediones (TZDs) and ABA showed the most favorable binding energy, thereby indicating the highest probability of binding to LANCL2.

Materials and methods

Template selection and model building

Template selection is a critical step in homology modeling. The amino acid sequence of LANCL2 (*Homo sapiens*) was obtained from the protein database at the National Center for Biotechnology Information (NCBI, http://www.ncbi.nlm.nih.gov/). LANCL2 includes 450 amino acid residues and its accession number is NP_061167. To determine if structural templates in addition to LANCL1 [12] were available, sequence searching was done. BLASTp (protein–protein BLAST) and the BLOSUM62 scoring matrix were applied to search for potential templates for LANCL2 in the non-redundant protein sequence database [13]. Gap existence was penalized 11 from an overall score and each gap extension was deducted 1. Based on this analysis, LANCL1 (*H. sapiens*) was identified as the only template for modeling LANCL2 (*H. sapiens*).

To further verify whether LANCL1 is an appropriate template, multiple sequence alignment (MSA) was used to analyze conserved residues and potential sequence motifs of LANCL2. Five target sequences (LANCL2) and five template sequences (LANCL1) from different organisms were selected from the protein database in NCBI. MSA was performed using the CLUSTALW package in Biology Workbench applying the default parameters to insure proper alignment between the template and target [14, 15]. The high sequence identity (54%) and sequence similarity (71%) indicate the suitability of LANCL1 as a template for LANCL2 in homology modeling (Fig. 1).

The three-dimensional structure of LANCL2 was constructed by using the SWISS-MODEL Workspace [16]. The template used was the X-ray structure of LANCL1 (2.6 Å resolution, PDB entry code 3E6UC) [17].

Model assessment and refinement

Model quality was assessed employing two types of assessment tools, ANOLEA [18] and PROCHECK [19]. Local quality model estimation (ANOLEA) describes the quality of different fragments of the same model. Energies of each residue were calculated based on an atomic empirical mean force potential. The stereochemical check (PROCHECK) was applied to determine if the φ and ψ dihedral angles were in available zones of the Ramachandran plot.

After initial model assessment, an energy minimization (EM) procedure was carried out with the GROMACS 4.0.5

```
 Score =  487 bits (1253),  Expect = 1e-135, Method: Compositional matrix adjust.
 Identities = 231/426 (54%), Positives = 304/426 (71%), Gaps = 27/426 (6%)

Query  19   MEERAFVNPFPDYEAAAGALLASGAAEETGCVRPPATTDEPGLPFHQDGKIIHNFIRRIQ  78
            M +RAF NP+ DY  +    LA G                    F   G++   F +R+
Sbjct  13   MAQRAFPNPYADYNKS----LAEGY-------------------FDAAGRLTPEFSQRLT  49

Query  79   TKIKDLLQQMEEGLKTADPHDCSAYTGWTGIALLYLQLYRVTCDQTYLLRSLDYVKRTLR  138
             KI++LLQQME GLK+ADP D + YTGW GIA+LYL LY V  D  YL  +  YVK++L
Sbjct  50   NKIRELLQQMERGLKSADPRDGTGYTGWAGIAVLYLHLYDVFGDPAYLQLAHGYVKQSLN  109

Query  139  NLNGRRVTFLCGDAGPLAVGAVIYHKLRSDCESQECVTKLLQLQRSVVCQESDLPDELLY  198
             L  R +TFLCGDAGPLAV AV+YHK+ ++ ++++C+T+L+ L +     +   P+E+LY
Sbjct  110  CLTKRSITFLCGDAGPLAVAAVLYHKMNNEKQAEDCITRLIHLNKI----DPHAPNEMLY  165

Query  199  GRAGYLYALLYLNTEIGPGTVCESAIKEVVNAIIESGKTLSREERKTERCPLLYQWHRKQ  258
            GR GY+YALL++N   G   + +S I+++   I+ SG+ L+R+   T + PL+Y+W+++
Sbjct  166  GRIGYIYALLFVNKNFGVEKIPQSHIQQICETILTSGENLARKRNFTAKSPLMYEWYQEY  225

Query  259  YVGAAHGMAGIYYMLMQPAAKVDQETLTEMVKPSIDYVRHKKFRSGNYPSSLSNETDRLV  318
            YVGAAHG+AGIYY LMQP+ +V Q  L  +VKPS+DYV   KF SGNYP  + +  D LV
Sbjct  226  YVGAAHGLAGIYYYLMQPSLQVSQGKLHSLVKPSVDYVCQLKFPSGNYPPCIGDNRDLLV  285

Query  319  HWCHGAPGVIHMLMQAYKVFKEEKYLKEAMECSDVIWQRGLLRKGYGICHGTAGNGYSFL  378
            HWCHGAPGVI+ML+QAYKVF+EEKYL +A +C+DVIWQ GLL+KGYG+CHG+AGN Y+FL
Sbjct  286  HWCHGAPGVIYMLIQAYKVFREEKYLCDAYQCADVIWQYGLLKKGYGLCHGSAGNAYAFL  345

Query  379  SLYRLTQDKKYLYRACKFAEWCLDYGAHGCRIPDRPYSLFEGMAGAIHFLSDVLGPETSR  438
            +LY LTQD KYLYRACKFAEWCL+YG HGCR PD P+SLFEGMAG I+FL+D+L P  +R
Sbjct  346  TLYNLTQDMKYLYRACKFAEWCLEYGEHGCRTPDTPFSLFEGMAGTIYFLADLLVPTKAR  405

Query  439  FPAFEL  444
            FPAFEL
Sbjct  406  FPAFEL  411
```

Fig. 1 Sequence alignment of LANCL2 (*Homo sapiens*) with LANCL1 (*H. sapiens*) using the BLASTp algorithm. The Query is the LANCL2 amino acid sequence, while the Sbjct is the LANCL1 sequence. Identical residues are showed in the line between Query and Sbjct. A plus (+) indicates a conserved substitution

software suite using an all-atom force field (OPLS-AA) [20, 21]. The purpose of an EM procedure is to reduce steric clashes in the input structure and to obtain lower potential energy in the system and therefore a more stable structure. The EM algorithm used was steepest descent minimization [22]. The maximum force to stop minimization, energy step size and maximum number of minimization steps to perform were set to 1,000 KJ mol^{-1} nm^{-1}, 0.01 and 50,000, respectively. The final LANCL2 model was superimposed on the crystal structure of LANCL1 to check the structural differences between the homology model and template by using the RAPIDO program [23].

Ligand structure

The three-dimensional structure of ABA was downloaded from PubChem, a database of chemical molecules maintained by the NCBI [24]. The compound ID of ABA is 5280896 and its molecular formula is $C_{15}H_{20}O_4$.

Molecular docking

The docking of ABA into the LANCL2 model was performed with AutoDock (version 4.2) [25]. AutoDockTools, the graphical front-end for AutoDock and AutoGrid, was used to set up, run and analyze AutoDock dockings. The Lamarckian genetic algorithm (LGA) was used in AutoDock as the search method to perform automated molecular dockings [26]. Default parameters were applied, except for the number of GA runs, population size and maximum number of evaluations, which were set to 100, 250 and 25,000,000, respectively.

In order to identify potential binding sites of ABA on LANCL2, the docking procedure was performed in two steps. At first, the docking was applied to the whole protein target, with a grid covering the whole surface of the protein. AutoDock can be used when the location of the binding site is unknown. This is often referred to as “blind docking”, when all that is known is the structure of the ligand and the macromolecule [27–32]. To search the entire surface of the protein of interest, very large grid maps were created using AutoGrid, with the maximum number of points in each dimension. The grid was a 126 Å cube with grid points separated by 0.59 Å and centered at the middle of the protein. This grid was big enough to cover the entire surface of LANCL2. Then the preliminary dockings with AutoDock were performed to search for particular regions of LANCL2 that were preferred by ABA. In the second round of docking, smaller grids were built around potential binding sites. The X, Y, Z dimensions of grid were set to 70 Å with grid points separated by 0.375 Å.

Analyzing results of docking

The search for the best ways to fit ABA into LANCL2 using AutoDock resulted in docking log files that contained detailed records of docking. These log files were read into ADT to analyze the results of docking. The similarity of docked structures was measured by computing the root-mean-square-deviation (RMSD) between the coordinates of

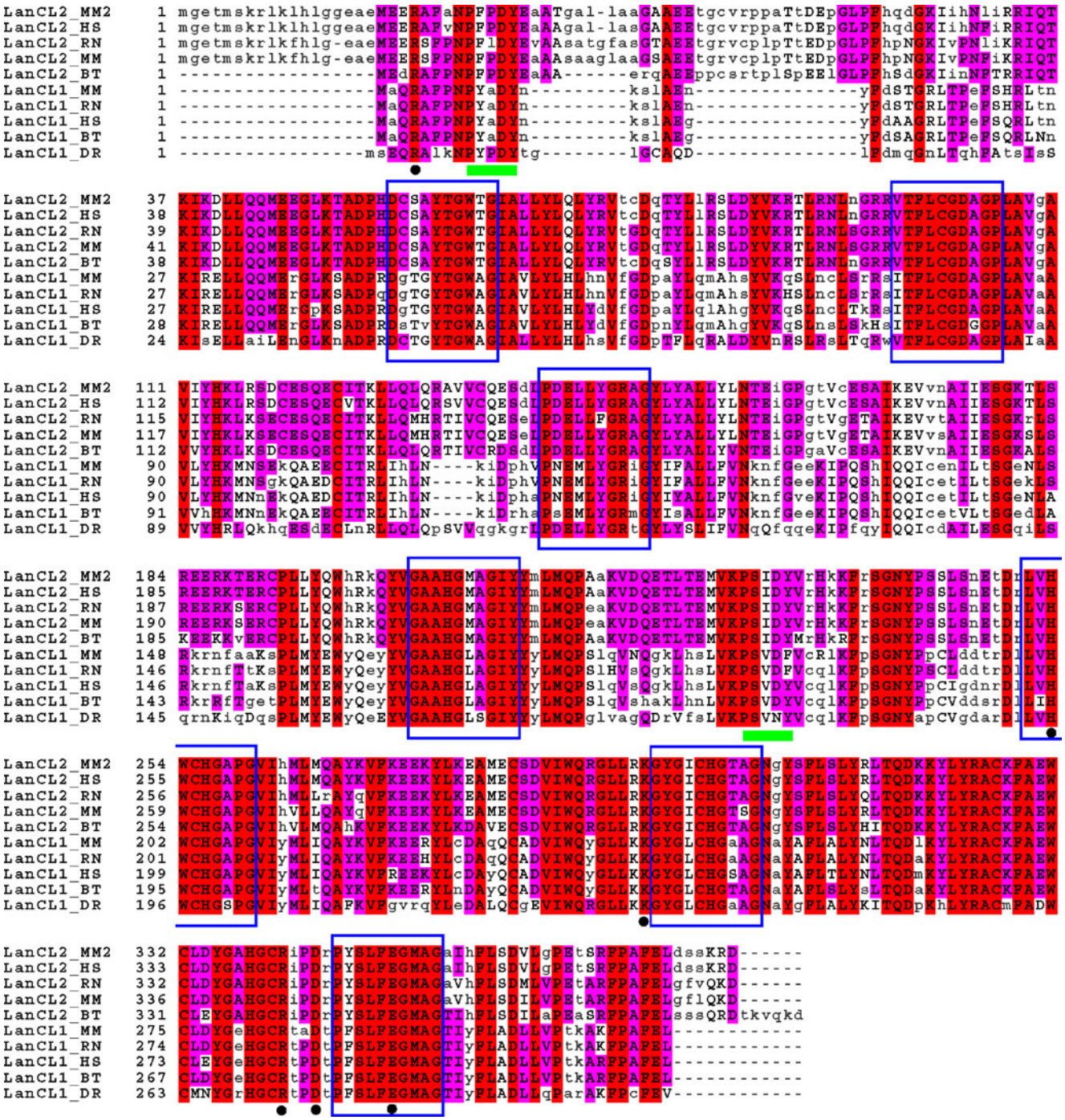

Fig. 2 Multiple sequence alignment of selected LanC proteins. LANCL2_MM2: *Macaca mulatta*; LANCL2_HS: *Homo sapiens*; LANCL2_RN: *Rattus norvegicus*; LANCL2_MM: *Mus musculus*; LANCL2_BT: *Bos taurus*; LANCL1_MM: *Mus musculus*; LANCL1_RN: *R. norvegicus*; LANCL1_HS: *H. sapiens*; LANCL1_BT: *B. taurus*; LANCL1_DR: *Danio rerio*. Completely conserved residues in the listed sequences are highlighted with a *red* background. Identical residues are highlighted with a *magenta* background. Different residues are shown in lower-case letters. Seven conserved GxxG motifs and corresponding loop bulges are outlined by *blue boxes*. Canonical SH3-binding motifs are underlined with *green lines*. Positions of GSH-binding residues in LANCL1 are denoted by *black dots*

the atoms and creating clustering of the conformations based on these RMSD values. In most cases the first cluster was also the largest cluster found. The lowest binding energy conformation in the first cluster was considered as the most favorable docking pose. Binding energies that are reported represent the sum of the total intermolecular energy, total internal energy and torsional free energy minus the energy of the unbound system.

Fig. 3 Overall structure of LANCL2. The homology model of human LANCL2 is shown in *New Cartoon* representation with coloring according to secondary structure. *Purple* Alpha helix, *blue* other helix, *yellow* bridge_beta, *cyan* turn, *green* coil. The image was rendered in VMD

Results and discussion

Template search

Homology modeling relies on establishing an evolutionary relationship between the sequence of a protein of interest and other members of the protein family whose structures have been solved experimentally by X-ray crystallography or NMR. For this reason, the major limitation of this technique is the availability of homologous templates. In most cases, two proteins with more than 35% sequence identity are likely to be homologous [33]. The crystal structure of human LANCL1 (3E6U), which shares 54% sequence identity with LANCL2, has been reported by Zhang and colleagues [12].

To further verify whether functionally important residues and motifs are conserved, multiple sequence alignment was performed between five LANCL1 and five LANCL2 sequences from different organisms (Fig. 2). The alignment showed all LANCL2 sequences also had seven conserved GxxG motifs similar to LANCL1. These seven conserved GxxG-containing motifs are considered to be a signature feature of the LANCL family of proteins because they are absent in other double helix barrel proteins [12]. Furthermore, canonical SH3-binding motifs and GSH-binding residues of LANCL1 also appeared to be highly conserved in the five LANCL2 sequences. All of these findings suggest that LANCL1 and LANCL2 are not only conserved in terms of sequence but are also functionally similar, thus homology modeling of LANCL2 using the LANCL1 structure as template is appropriate.

Model building

SWISS-MODEL Workspace was used to generate the homology model of LANCL2 according to the crystal structure of LANCL1 [16]. As expected, the predicted structure of LANCL2 consists of two layers of α-helical barrels consisting of 14 α-helices. The outer barrel is formed by seven helices that are parallel to one another, while the inner barrel is formed by seven helices that are also parallel to one another. The orientation of the two layer barrel helices is opposite, but both inner and outer barrels have a left-handed twist. The seven conserved GxxG-containing bulges are at the N-termini of the inner helices. These bulged loops reduce the entry size of the central cavity formed by the inner helix barrel. Therefore, LANCL2 is unlikely to use the central cavity as a ligand binding site. The structure of LANCL2 is shown in Fig. 3 [34].

Model assessment and refinement

Two levels of assessment were performed to determine the quality of the model generated. The atomic empirical mean force potential ANOLEA was used to assess packing quality of the models [18]. ANOLEA performs energy calculations on a protein chain, evaluating the "non-local environment" (NLE) of each heavy atom in the molecule. In the ANOLEA plot, the y-axis of the plot represents the energy for each amino acid of the protein chain. Negative energy values (in green) represent a favorable energy environment whereas positive values (in red), an unfavorable energy environment for a given amino acid. Most amino acid residues in the LANCL2 model appeared in a favorable environment (Fig. 4). The PROCHECK suite of programs assesses the stereochemical quality of a given protein structure [19]. The Ramachandran plot from PROCHECK also indicated the good quality of the model, with 85.3% of φ,ψ angles in the favored core region, 13.7% in allowed regions, and only 0.5% of residues in generously allowed regions and 0.5% in disallowed regions (Fig. 4).

To improve and verify the stability of the initial structure, an energy minimization procedure was applied to the LANCL2 model [22]. The energy minimization procedure was set to stop when the maximum force reached 1,000 KJ mol^{-1} nm^{-1}. The potential energy in the system decreased in the energy minimization procedure. At the same time, the RMSD of LANCL2 structure relative to the starting structures increased only 0.03 nm. These results show that after the energy minimization procedure, the LANCL2 structure became more stable. Finally, the homology model of LANCL2 improved by the EM procedure and crystal structure of template (LANCL1) were compared using RAPIDO, a superposition webserver

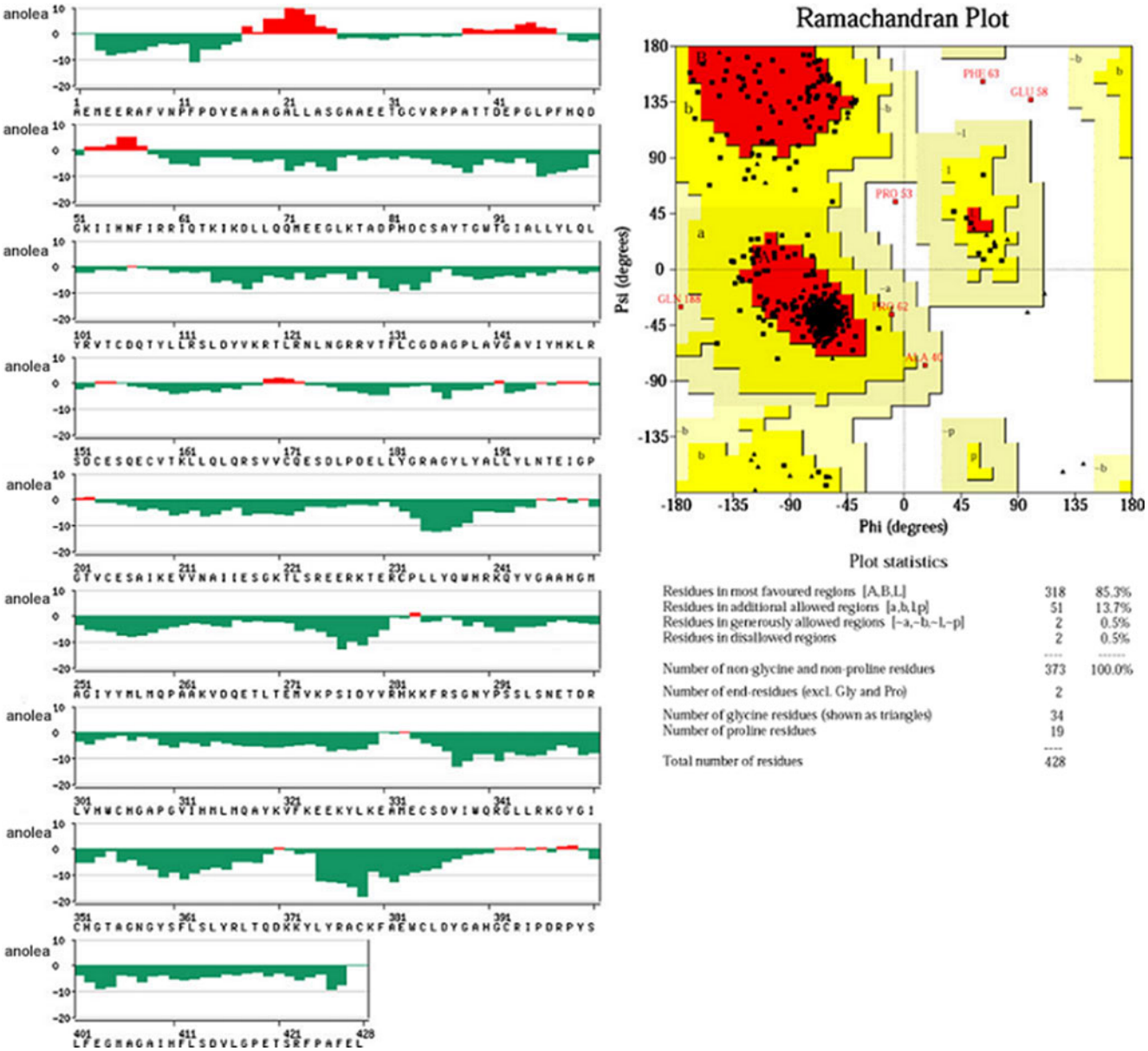

Fig. 4 ANOLEA plot (*left*) and Ramachandran plot (*right*) of modeled LANCL2. In the ANOLEA plot, negative values (*green*) indicate residues in a favorable environment and positive values (*red*) indicate residues in an unfavorable environment. In the Ramachandran plot, the favored and most favored region is *yellow* and *red* respectively; *pale yellow* is the generously allowed and disallowed regions are *white*

[23]. Figure 5 shows the LANCL2 model is very similar to the LANCL1 structure, including two layers of α-helical barrels and seven GxxG-containing bulges. The RMSD between the LANCL2 model and LANCL1 structure is 0.47 Å. On the basis of the above analysis, the homology model of LANCL2 improved by the EM procedure was employed for the following docking study.

Molecular docking and result analysis

The AutoDock program is one of the most widely cited docking programs in the research community, owing its efficiency to the use of the LGA and a grid-based scoring function comprising several terms, including dispersion/repulsion energy, directional hydrogen bonding, screened Coulomb potential electrostatics, a volume-based solvation term, and a weighted sum of torsional degrees of freedom to estimate the entropic cost of binding [32]. Furthermore, it can identify potential binding sites of a ligand on a protein using blind docking, without the information about binding sites. In addition, full consideration of flexibility of ligands during the docking procedure makes AutoDock an appropriate tool for binding site identification. The docking of ABA with LANCL2 was performed in two steps.

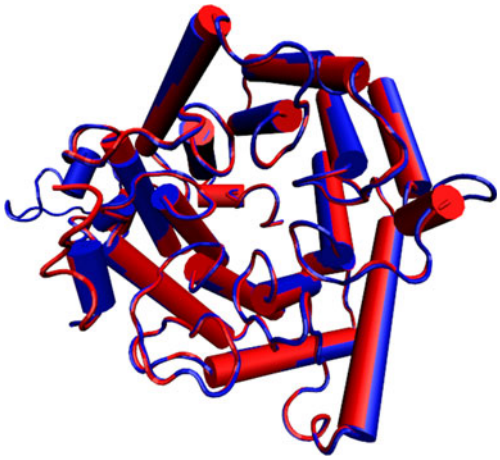

Fig. 5 Superposition of the LANCL2 model and the LANCL1 template structures. *Blue* LANCL2, *red* LANCL1, *cylinders* helices, *tube* random coil

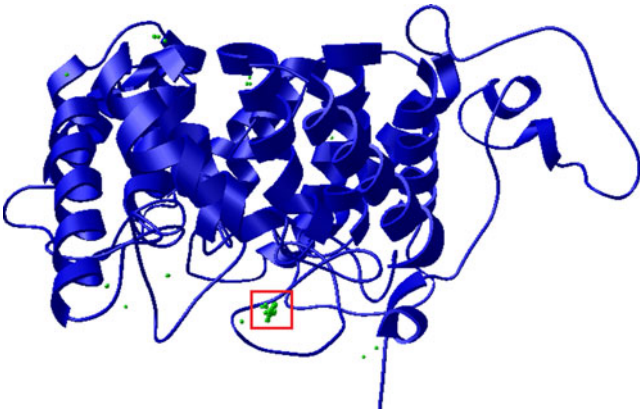

Fig. 7 Overview of the distribution of conformations. Each docked conformation is represented by a *green* sphere placed at the average position of the coordinates of all the atoms in that conformation. The binding site with the most poses of ABA is outlined by the *red box*

In the first step, the blind docking approach was used in order to identify the potential binding sites of LANCL2. The grid generated by AutoGrid was big enough to cover the entire surface of LANCL2. The 100 resulting conformations of ligands were clustered with an RMSD cluster tolerance of 2.0 Å. The clustering plot revealed that 58% of the poses of ABA are located in the first cluster with a mean binding energy of −6.70 kcal mol^{-1} (Fig. 6). Examination of the distribution of the binding site on the LANCL2 implies that ABA shows preferential binding to the loop regions of LANCL2, which is consistent with our prediction about the substrate-binding site of LANCL2 (Fig. 7). This region on the LANCL2 with the high population of clusters was considered as the potential binding site for ABA. Figure 8 shows ABA bound inside a pocket in LANCL2. The binding pocket was surrounded by TYR179, LYS284, PHE285, PRO291, ASN296 and SER295. LYS 283 was located in the bottom of the pocket. Two hydrogen bonds formed between the nitrogen atom in the side chain of LYS283 and two hydroxyl groups of ABA that positioned ABA deep in the pocket and increased the affinity of ABA for LANCL2 (Fig. 8).

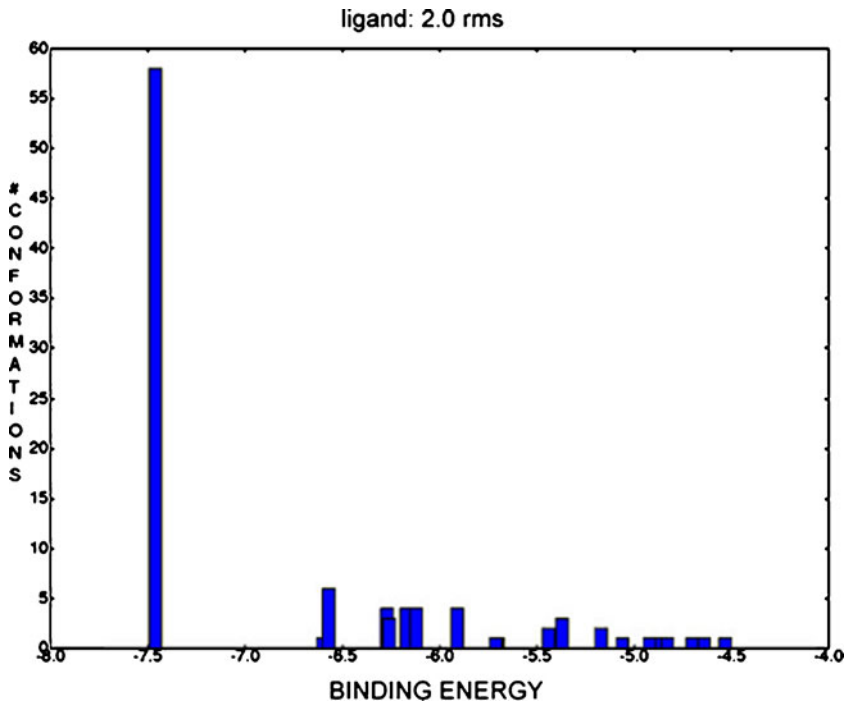

Fig. 6 Representations of docked results by clustering histogram. The 100 resulting conformations of ligands were clustered with root-mean-square-deviation (RMSD) cluster tolerance of 2.0 Å. *Abscissa* represents the lowest binding energy in each cluster

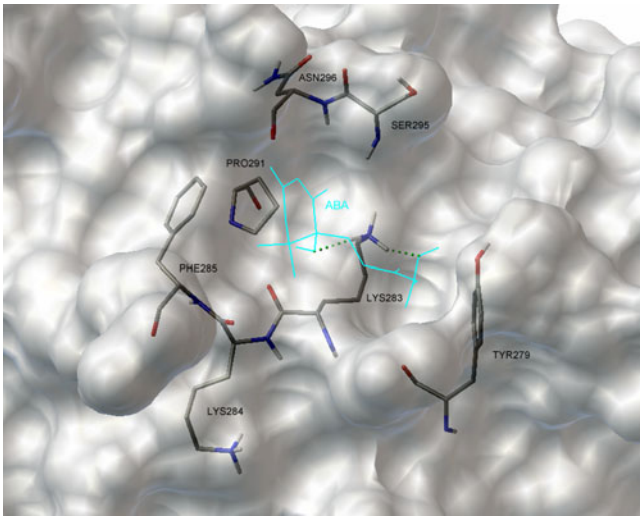

Fig. 8 Representative binding modes of the most stable docked orientation of abscisic acid (ABA) with LANCL2. LANCL2 is shown in a *molecular surface model*. ABA is shown by a *cyan stick model*, and selected residues of LANCL2 are depicted by *gray stick models*. Hydrogen bonds are shown as *dashed green lines*. Amino acid residues surrounding ABA are labeled

In the second step (focused docking), ABA was docked into the binding site previously found. The use of an increased grid resolution focusing on the predicted binding site allows more focused searching and better evaluation of the protein-ligand interactions, and consequently lower binding energies are obtained with respect to the blind docking (Fig. 9). Comparisons of docking results were performed between blind docking and focused docking (Table 1).

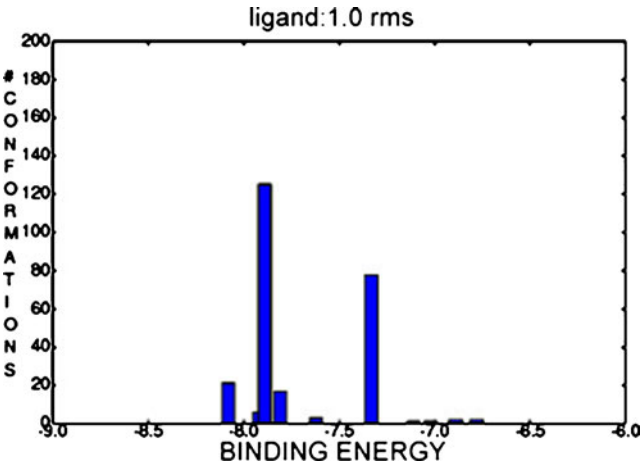

Fig. 9 Clustering histogram (left). The 256 resulting conformations of ligands were clustered with RMS cluster tolerance of 1.0 Å. *Abscissa* represents the lowest binding energy in each cluster

Table 1 Comparison docking results between blind docking and focused docking

	Cluster number	Lowest binding energy	Mean binding energy in the first cluster
Blind docking	20	−7.46 kcal/mol	−6.70 kcal/mol
Focused docking	10	−8.08 kcal/mol	−7.92 kcal/mol

Docking test of other PPAR γ agonists on LANCL2

In order to determine whether other PPAR γ agonists might also bind to LANCL2, we docked several small molecules, including rumenic acid, punicic acid, catalpic acid, eleostearic acid, calendic acid, jacaric acid, pioglitazone and rosiglitazone, to LANCL2 using the blind docking method. Docking results are displayed in Table 2 according to the lowest binding energy of these chemicals. Compared to the other molecules, pioglitazone and rosiglitazone showed better binding ability to LANCL2 with lower binding energy. These compounds belong to the TZD class of T2D drugs and, in contrast to ABA, are known to bind to the LBD of PPAR γ. Docking results showed that pioglitazone and rosiglitazone could bind to the same binding site as ABA on LANCL2 (Fig. 10). On the basis of this result, we propose that LANCL2 is not just necessary for transduction of the ABA signal into cell-specific functional responses, but it may also be one important membrane receptor for a series of antidiabetic drugs that act by activating PPAR γ. Further studies are in process to verify our prediction.

Conclusions

The aim of this study was to build a three-dimensional structural model of LANCL2 and to identify the binding site of ABA in LANCL2. In the present work we generated the model of LANCL2 by homology modeling, to which ABA was docked using the blind docking method. By focused docking, the best binding site of ABA with low binding energy was identified, which indicates that LANCL2 may serve as the membrane receptor for ABA. Additionally, pioglitazone and rosiglitazone bound to the same site as ABA on LANCL2. On the basis of these findings, we propose a novel mechanism by which PPAR γ agonists can elicit their biological effects. Our LANCL2 model will be applicable for virtual screening of novel compounds for the treatment of T2D and other inflammatory diseases.

Table 2 Docking results of small molecules to LANCL2, ranked by the lowest binding energy

Common Name	Chemical Name	Chemical Structure	Lowest Binding Energy (kcal/mol)
abscisic acid	[*S*-(*Z*,*E*)]-5-(1-Hydroxy-2,6,6 -trimethyl-4-oxo-2-cyclohexen-1-yl)-3-methyl-2,4-pentanedienoic acid	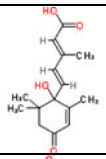	-7.46
rosiglitazone	(RS)-5-[4-(2-[methyl(pyridin-2-yl)amino]ethoxy)benzyl]thiazolidine-2,4-dione	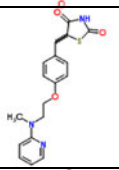	-7.95
pioglitazone	(RS)-5-(4-[2-(5-ethylpyridin-2-yl)ethoxy]benzyl) thiazolidine-2,4-dione	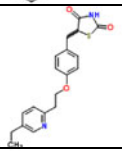	-7.08
α-Calendic acid	(8E,10E,12Z)-octadeca-8,10,12-trienoic acid	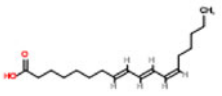	-5.79
catalpic acid	(9Z,11Z,13E)-octadeca-9,11,13-trienoic acid	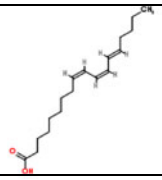	-5.72
β-Calendic acid	(8E,10E,12E)-octadeca-8,10,12-trienoic acid	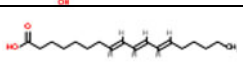	-5.65
t10,c12 conjugated linoleic acid	(10E,12Z)-octadeca-9,11-dienoic acid	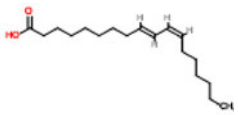	-5.40
β -eleostearic acid	(9E,11E,13E)-octadeca-9,11,13-trienoic acid	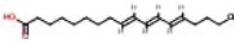	-5.28
α -eleostearic acid	(9Z,11E,13E)-octadeca-9,11,13-trienoic acid	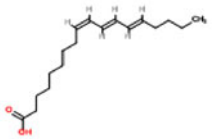	-5.21
punicic acid	(9Z,11E,13Z)-octadeca-9,11,13-trienoic acid	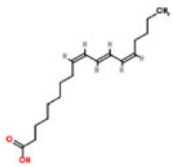	-5.18
jacaric acid	(8E,10Z,12E)-octadeca-8,10,12-trienoic acid	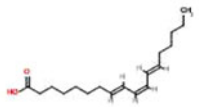	-5.09
c9, t11 conjugated linoleic acid	(9Z,11E)-octadeca-9,11-dienoic acid	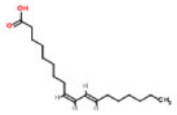	-4.98

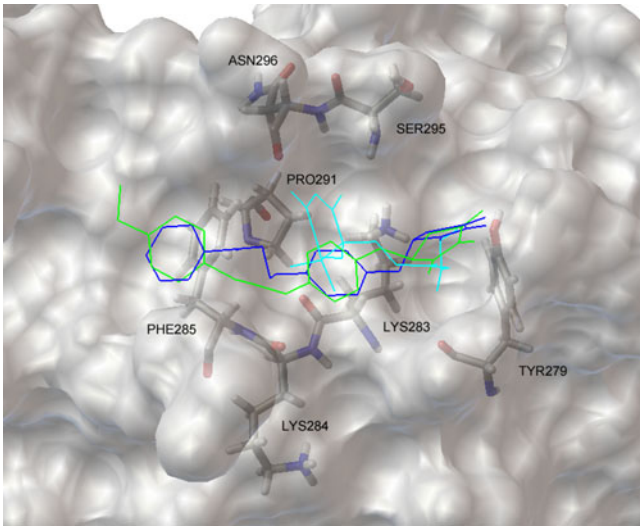

Fig. 10 Representation of the binding modes of ABA and thiazolidinedione (TZD) on LANCL2. *Cyan* ABA, *green* pioglitazone, *blue* rosiglitazone. LANCL2 is shown in a *molecular surface model*. Selected residues of LANCL2 are depicted by *stick-and-ball models* and colored by atom types (*red* oxygen, *blue* nitrogen, *white* hydrogen). This figure illustrates that ABA and TZDs may bind to the same site on LANCL2

Acknowledgments Supported by award number 5R01AT4308 of the National Center for Complementary and Alternative Medicine at the National Institutes of Health awarded to J.B.-R., European Commission grant number 224836, the Ramon y Cajal Program and funds from the Nutritional Immunology and Molecular Nutrition Laboratory.

References

1. Kumar V, Robbins SL, Cotran RS (2005) Pathologic basis of disease. Elsevier Saunders, Philadelphia
2. Inzucchi SE, Sherwin RS (2005) The prevention of type 2 diabetes mellitus. Endocrinol Metab Clin N Am 34:199–219
3. Defronzo RA (1999) Pharmacologic therapy for type 2 diabetes mellitus. Ann Intern Med 133:73–74
4. Defronzo RA, Ratner RR, Han J et al (2005) Effects of exenatide (exendin-4) on glycemic control and weight over 30 weeks in metformin-treated patients with type 2 diabetes. Diab Care 28:1092–1100
5. Rang HP, Dale MM, Ritter JM, Moore PK (2003) Pharmacology. Churchill Livingstone, New York
6. Nesto RW, Bell D, Bonow RO et al (2003) Thiazolidinedione use, fluid retention, and congestive heart failure: a consensus statement from the American Heart Association and American Diabetes Association. October 7, 2003. Circulation 108:2941–2948
7. Lewis SN, Bassaganya-Riera J, Bevan DR (2010) Virtual Screening as a Technique for PPAR Modulator Discovery. PPAR Res. Article ID 861238, 10 pages, doi:10.1155/2010/861238
8. Bassaganya-Riera J, Skoneczka1 J, Kingston DGJ et al (2010) Mechanisms of action and medicinal applications of abscisic acid. Curr Med Chem 17:467–478
9. Guri A, Hontecillas R, Ferrer G et al (2008) Loss of PPAR gamma in immune cells impairs the ability of abscisic acid to improve insulin sensitivity by suppressing monocyte chemoattractant protein-1 expression and macrophage infiltration into white adipose tissue. J Nutr Biochem 19(4):216–228
10. Sturla L, Fresia C, Guida L et al (2009) LANCL2 is necessary for abscisic acid binding and signaling in human granulocytes and in rat insulinoma cells. J Biol Chem 284:28045–28057
11. Landlinger C, Salzer U, Prohaska R (2006) Myristoylation of human LanC-like protein 2 (LANCL2) is essential for the interaction with the plasma membrane and the increase in cellular sensitivity to adriamycin. Biochim Biophys Acta 1758:1759–1767
12. Zhang W, Wang L, Liu Y et al (2009) Structure of human lanthionine synthetase C-like protein 1 and its interaction with Eps8 and glutathione. Genes Dev 23:1387–1392
13. Altschul SF, Gish W, Miller W (1990) Basic local alignment search tool. J Mol Biol 215:403–410
14. Thompson JD, Higgins D, Gibson TJ (1994) CLUSTAL W: improving the sensitivity of progressive multiple sequence alignment through sequence weighting, position-specific gap penalties and weight matrix choice. Nucleic Acids Res 22:4673–4680
15. Subramaniam S (1998) The Biology Workbench-a seamless database and analysis environment for the biologist. Proteins 32:1–2
16. Arnold K, Bordoli L, Kopp J, Schwede T (2006) The SWISS-MODEL workspace: a web-based environment for protein structure homology modelling. Bioinformatics 22:195–201
17. Berman HM, Westbrook J, Feng Z (2000) The protein data bank. Nucleic Acids Res 28:235–242
18. Melo F, Feytmans E (1998) Assessing protein structures with a non-local atomic interaction energy. J Mol Biol 277:1141–1152
19. Laskowski RA, MacArthur MW, Moss D, Thornton JM (1993) PROCHECK: a program to check the stereochemical quality of protein structures. J Appl Cryst 26:283–291
20. Hess B, Kutzner C, van der Spoel D, Lindahl E (2008) GROMACS 4: algorithms for highly efficient, load-balanced, and scalable molecular simulation. J Chem Theory Comput 4:435–447
21. Jorgensen WL, Tirado-Rives J (1988) The OPLS force field for proteins. Energy minimizations for crystals of cyclic peptides and crambin. J Am Chem Soc 110:1657–1666
22. Wiberg KB (1965) A scheme for strain energy minimization. J Am Chem Soc 87:1070–1078
23. Mosca R, Schneider T (2008) RAPIDO: a web server for the alignment of protein structures in the presence of conformational changes. Nucleic Acids Res 36:W42–W46
24. Wang YL, Xiao J, Suzek TO et al (2009) PubChem: a public information system for analyzing bioactivities of small molecules. Nucleic Acids Res 37:W623–W633
25. Morris GM, Huey R, Lindstrom W et al (2009) AutoDock4 and AutoDockTools4: automated docking with selective receptor flexibility. J Comput Chem 30:2785–2791
26. Morris GM, Goodsell D, Halliday RS et al (1998) Automated docking using a Lamarckian genetic algorithm and an empirical binding free energy function. J Comput Chem 19:1639–1662
27. Hetényi C, van der Spoel D (2002) Efficient docking of peptides to proteins without prior knowledge of the binding site. Protein Sci 11:1729–1737
28. Hetényi C, van der Spoel D (2006) Blind docking of drug-sized compounds to proteins with up to a thousand residues. FEBS Lett 580:1447–1450
29. Iorga B, Herlem D, Barre E, Guillou C (2006) Acetylcholine nicotinic receptors: finding the putative binding site of allosteric modulators using the "blind docking" approach. J Mol Model 12:366–372
30. Bikádi Z, Hazai E, Zsila F, Lockwood SF (2006) Molecular modeling of non-covalent binding of homochiral (3S, 3′S)-

astaxanthin to matrix metalloproteinase-13 (MMP-13). Bioorg Med Chem 14:5451–5458
31. Hazai E, Bikádi Z, Zsila F, Lockwood SF (2006) Molecular modeling of the non-covalent binding of the dietary tomato carotenoids lycopene and lycophyll, and selected oxidative metabolites with 5-lipoxygenase. Bioorg Med Chem 14:6859–6867
32. Kovács M, Toth J, Hetényi C, Málnási-Csizmadia A, Sellers JR (2004) Mechanism of blebbistatin inhibition of myosin II. J Biol Chem 279:35557–35563
33. Rost B (1999) Twilight zone of protein sequence alignments. Protein Eng 12:85–94
34. Humphrey W, Dalke A, Schulten K (1996) VMD: visual molecular dynamics. J Mol Graph 14(1):33–38